Arabian Journal for Science and Engineering
https://doi.org/10.1007/s13369-022-07307-1

RESEARCH ARTICLE-CHEMISTRY

Paracetamol and Ibuprofen Removal from Aqueous Phase Using a Ceramic-Derived Activated Carbon

Amalia L. Bursztyn Fuentes[1,2] · Damián E. Benito[3,4] · María L. Montes[4,5] · Alberto N. Scian[3,4] · M. Barbara Lombardi[3,4]

Received: 23 June 2022 / Accepted: 20 September 2022

Abstract
Emerging pollutants, including pharmaceuticals and personal care products, have been detected in surface and groundwaters. The adsorption of paracetamol and ibuprofen, two widespread drugs, has been studied in aqueous medium, using a ceramic-derived carbon (CeDC) and a commercial activated carbon (CoAC). CeDC yielded a BET surface area of 895 $m^2\ g^{-1}$, a bimodal pore size distribution (13.2 and 35 nm) and a total pore volume of 1.99 $cm^3\ g^{-1}$. CoAC had an approximate surface area of 1000 $m^2\ g^{-1}$, a homogeneous pore size distribution and a total pore volume of 0.42 $cm^3\ g^{-1}$. Kinetic and equilibrium tests were carried out in batch systems to study the materials' sorption performances. The intraparticle diffusion model best fitted the experimental kinetic data. The maximum ibuprofen sorption capacities were 120 mg g^{-1} and 133 mg g^{-1} for CoAC and CeDC, respectively, whereas no major differences on the maximum paracetamol sorption capacities (qm) were observed among the sorbents (150–159 mg g^{-1}). Therefore, CeDC, synthesized easily from a ceramic composite, improved time and sorption capacity of paracetamol and ibuprofen compared to the commercial activated carbon, indicating the potential of the developed carbon as an emerging pollutant sorbent material.

Keywords Paracetamol · Ibuprofen · Activated carbon · Ceramic composite · Sorption

1 Introduction

Nowadays, a lot of research is being conducted on emerging pollutants, as they are a group of chemical substances increasingly being found in surface and groundwater. Their detection, even at trace levels, has been facilitated by modern analytical instrumentation [1]. Among these pollutants, pharmaceuticals and personal care products are of major concern because they are the most frequently detected compounds, due to their massive consumption [2]. Although they are present at very low concentrations (down to ng L^{-1}), the average world annual consumption of pharmaceuticals is of 15 g per capita, reaching up to 50–150 g in developed countries [2, 3, 4]. This can imply severe risks to human and environmental health, given that these compounds are usually bioactive, bioaccumulative and persistent [5].

Activated carbons have been widely used to remove several pollutants from aqueous phase such as dyes [6], heavy metals [7], pesticides [8] and pharmaceutical products [9, 10, 11, 12]. Paracetamol and ibuprofen are widespread analgesics, anti-inflammatory drugs that do not require, in many countries, medical prescription [13]. These drugs have been detected in wastewater treatment plants [14], and concentrations are expected to rise given that the home treatment of early COVID-19 symptoms (i.e., fever) has promoted the consumption of certain drugs, particularly paracetamol [15, 16].

The aim of this article was to study the performance of a ceramic-derived activated carbon on the removal of

✉ Amalia L. Bursztyn Fuentes
amalbf@agro.uba.ar; albursztyn@untdf.edu.ar

1 Instituto de Ciencias Polares, Ambiente y Recursos Naturales (ICPA), Universidad Nacional de Tierra del Fuego, Yrigoyen 879, 9410 Ushuaia, Argentina

2 Centro Austral de Investigaciones Científicas (CADIC, CONICET), Bernardo Houssay 200, 9410 Ushuaia, Argentina

3 Centro de Tecnología de Recursos Minerales y Cerámica (CETMIC, CIC-CONICET-UNLP), Cno. Parque Centenario 2499-2599, 1897 M.B. Gonnet, Argentina

4 Facultad de Ciencias Exactas, Universidad Nacional de La Plata, 47 and 115, 1900 La Plata, Argentina

5 Instituto de Física La Plata (IFLP, CONICET), Diag. 113 and 64, 1900 La Plata, Argentina

Published online: 03 October 2022

paracetamol and ibuprofen from liquid phase. The synthesized material was texturally characterized, and its sorption capacities were assessed. A commercial activated carbon was included as a reference material for comparison purposes.

2 Materials and Methods

2.1 Activated Carbons

Two activated carbons were studied. The ceramic-derived carbon, CeDC, is a carbon produced from a SiO_2–C composite prepared via sol–gel method according to Benito et al. [17]. Briefly, the composite was prepared mixing commercial partially hydrolyzed tetraethyl orthosilicate, ethyl alcohol and phenolic-formaldehyde resin. After gelification, drying, curing and the thermal treatment, the carbonaceous network was isolated from the composite using an excess of HF 20% v/v for 24 h, and it was thermally treated at 450 °C to eliminate hexafluorosilicic acid. The other carbon was a commercial activated carbon (Clarimex S.A.), CoAC, used as reference material. According to the producer, it is a coconut-derived steam-activated carbon. Both activated carbons were ground and sieved between mesh #30 and #60 (ASTM), to obtain particles with sizes in the range 600–250 μm.

2.2 Characterization of the Materials

The carbon's morphology was studied with a scanning electron microscope (SEM, JEOL JCM6000). Samples were previously dried at 105 °C and kept in a desiccator at least 30 min before the analysis.

Nitrogen sorption isotherms were collected with a Micromeritics ASAP 2020 instrument at − 196 °C. The activated carbons were previously outgassed at 110 °C under secondary vacuum for at least 48 h. Specific surface area (S_{BET}) was estimated with the BET equation, in the adequate pressure range as recommended by IUPAC [18] and the total pore volume, *TPV* ($cm^3\ g^{-1}$), at $P/P_0 = 0.97$. The micropore volume, V_{micro} ($cm^3\ g^{-1}$), was determined from the application of the α-plot method to the N_2 adsorption isotherm. The mesopore volume, V_{meso} ($cm^3\ g^{-1}$), was calculated as the difference between *TPV* and V_{micro}.

Electro-kinetic potential measurements, automatically converted to zeta potential using the Smoluchowski equation, were determined with a Brookhaven 90Plus/Bi-MAS instrument. The measurements were taken at different pH values (2–11) on a previously sonicated suspension containing 1 g L^{-1} of material and KCl 1 mM solution. The suspension pH was adjusted adding HCl or KOH drops.

The oxygen surface group identification through Boehm titrations [19] was performed with a standardized procedure [20]. Briefly, 0.5 g of the carbon sample was added to 30 mL of each of the three 0.025 M reaction bases ($NaHCO_3$, Na_2CO_3 and NaOH) individually. Mixtures were shaken for 24 h and, after filtration, 10 mL aliquots were taken and acidified with 20–30 mL of standardized 0.025 M HCl. The acidified solutions were then bubbled with Ar (50 $cm^3\ min^{-1}$) for 2 h to eliminate dissolved CO_2 from solution and immediately titrated. All samples were titrated with standardized 0.025 M NaOH and phenolphthalein as indicator, continuous degassing was carried out, and the endpoints were determined potentiometrically. Overall basicity was determined also through back-titration using HCl 0.025 M.

X-ray diffraction (XRD) patterns were collected using a Philips PW 1710 diffractometer with CuKα radiation, operated at 40 kV and 30 mA, with counting time 10 s/step and 0.02° (2θ) step size. The main reflections were defined and contrasted with reference patterns.

Thermogravimetric and differential thermal analysis (DTA-TG) were simultaneously performed in air atmosphere, with a 10 °C min^{-1} heating rate up to 900 °C in alumina crucibles (Netzsch, Germany). The derivative curve of the TG (DTG) was also calculated.

2.3 Pollutants' Adsorption Studies

The materials were tested as paracetamol and ibuprofen sorbents in aqueous phase. Paracetamol (99.06%) and ibuprofen (99.9%) were produced and supplied by the Medicine Production Unit (*Unidad Productora de Medicamentos*) of the Faculty of Exact Sciences of the National University of La Plata (UNLP). Figure 1 presents the chemical structure of both compounds, including their corresponding molecular sizes. The pKa values for paracetamol and ibuprofen are 9.38 and 4.3–4.6, respectively. Single-component 200 mg L^{-1} stock solutions were prepared using the supplied drugs and ultrapure water. Ibuprofen dissolution was enhanced with 30% ethanol and sonication. The initial solution pH was 7.0 and 4.2 for paracetamol and ibuprofen, respectively. Therefore, in these conditions, both compounds do not present electric charge.

Preliminary tests were conducted to analyze the effect of pH and temperature on paracetamol and ibuprofen removal. To study the effect of pH, the materials were tested at 4.2, 7.0 and 9.0 (fixed conditions: initial concentration = 200 mg L^{-1}; solid-to-liquid ratio = 1 g L^{-1} and constant stirring at 25 °C). These pHs were attained by adding drops of HCl or KOH to the test solution accordingly before adding the carbons. To study the effect of temperature, the materials were tested at 4 °C, 15 °C and 25 °C, by controlling room temperature (fixed conditions: initial concentration = 200 mg L^{-1}; solid-to-liquid ratio = 1 g L^{-1}, constant stirring and no pH adjustment).

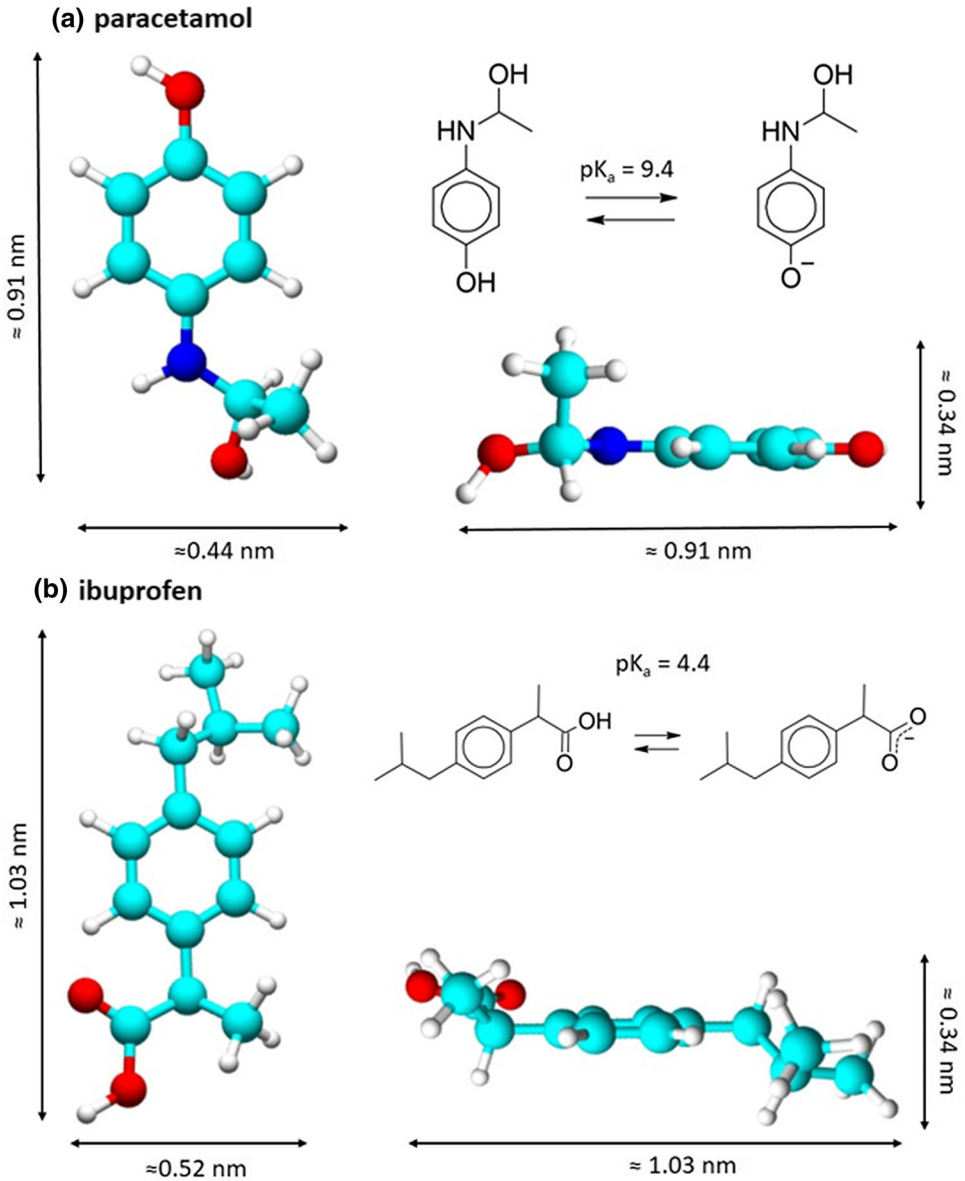

Fig. 1 Chemical structure, speciation and sizes of paracetamol (**a**) and ibuprofen (**b**)

Test solutions for preliminary tests, kinetics and equilibrium essays were prepared by dilution with ultrapure water of the stock solutions, accordingly.

2.3.1 Kinetic Studies

For kinetic studies, 15 mg of carbon and 15 mL of paracetamol or ibuprofen test solution (10 mg L^{-1}) were mixed in a glass flask that was introduced into a homogenizer and stirred at 30 rpm at 25 °C. After the desired contact time (from 5 min to 24 h), an aliquot was removed and the amount of pollutant remaining in the solution was determined by UV spectroscopy at 243 nm for paracetamol and 224 nm for ibuprofen (Lambda 35 UV/VIS Spectrometer, PerkinElmer). All tests were carried out in duplicate, and control batches without carbons were performed.

The sorption capacity, q_t, was calculated according to the following equation:

$$q_t = \frac{(C_0 - C_t)}{W} V \tag{1}$$

where q_t (mg g^{-1}) is the amount of pollutant removed at time t, C_0 (mg L^{-1}) is the initial concentration of pollutant, C_t (mg L^{-1}) is the concentration of pollutant at time t, V (L) is the volume of the solution, and W (g) is the weight of dry carbon sample.

Four different kinetics models have been used to describe the experimental data: pseudo-first-order (PFO) kinetic model [21], pseudo-second-order (PSO) kinetic model [22],

Table 1 Summary of the kinetic and equilibrium models fitted to the experimental data

Model	Expression
Kinetic models	
Pseudo-first order (PFO) [21]	$q_t = q_e\left(1-e^{-k_1 t}\right)$
Pseudo-second order (PSO) [22]	$q_t = \frac{q_e^2 k_2 t}{1+q_e k_2 t}$
Elovich [23]	$q_t = \frac{1}{\beta}(1+\ln\alpha\beta t)$
Intraparticle diffusion (IPD) [24]	$q_t = k_P t^{1/2} + C$
Equilibrium models	
Langmuir [25]	$q_e = \frac{K_L q_m C_e}{1+K_L C_e}$
Freundlich [26]	$q_e = K_F (C_e)^{1/n}$
Langmuir–Freundlich [27]	$q_e = \frac{q_m (K_a C_e)^n}{1+(K_a C_e)^n}$

General references: qt is the sorption capacity at time t (mg g^{-1}); qe is the sorption capacity at equilibrium (mg g^{-1}); k_1 (min^{-1}) is the kinetic rate constant of pseudo-first order; k_2 (g mg^{-1} min^{-1}) is the pseudo-second-order rate constant; α (mg g^{-1} min^{-1}) is Elovich equation constant; and β (g mg^{-1}) is the Elovich equation exponent; k_P is the IPD rate constant (mg/(g $min^{1/2}$)); and C is a constant for any experiment (mg g^{-1}). Langmuir: K_L (L mg^{-1}) is the Langmuir constant, and q_m(mg g^{-1}) is the monolayer adsorption capacity. Freundlich: K_F ($mg^{1-1/n}$ $L^{1/n}$ g^{-1}) is the Freundlich constant and n (dimensionless) is the Freundlich exponent. Langmuir–Freundlich: K_a (L mg^{-1}) is the model's constant, and n (dimensionless) is the heterogeneity factor

Elovich model [23] and intraparticle diffusion model (IPD) [24]. Table 1 summarizes the corresponding mathematical expressions. The PFO model is valid when adsorption follows the Henry law, with velocity controlled by the reaction at the adsorbent surface, and when a relatively high solid-to-liquid ratio is used. It also assumes that the adsorbent presents a homogeneous surface. The PSO model assumes that the adsorbate needs two free adjacent sites on the surface of the adsorbent and that the rate-limiting step may be chemisorption, not diffusion. The Elovich model proposes that the interaction occurs by means of chemical reactions between the adsorbent and the adsorbate. Finally, the IPD model assumes that the pollutant adsorption rate onto the material depends on the rate of mass transport processes (i.e., diffusion).

The selection of the most suitable model representing the experimental data was done considering the R^2 parameter and the normalized standard deviation, $\Delta g\%$, calculated according to Eq. 2 [28]:

$$\Delta g(\%) = 100 * \sqrt{\frac{\sum_{i=1}^{N}[(q_{e\mathrm{EXP}} - q_{e\mathrm{CAL}})/q_{e\mathrm{EXP}}]^2}{N-1}} \quad (2)$$

where $q_{e\mathrm{EXP}}$ (mg g^{-1}) is the experimental sorption capacity at equilibrium and q_{eCAL} (mg g^{-1}) is the calculated sorption capacity at equilibrium.

2.3.2 Equilibrium Tests

Sorption studies on CoAC and CeDC at equilibrium were carried out at 25 °C by varying the pollutants' initial concentrations (5 – 200 mg L^{-1}). After 24 h, to guarantee equilibrium, the suspensions were left to settle and an aliquot was taken for the measurement. Dilutions were performed, when necessary. Then, the concentration of paracetamol or ibuprofen remaining in solution at equilibrium (C_e) was determined, and the corresponding uptake (q_e) was calculated using Eq. (1). All experiments were performed in duplicate. The isotherms were modeled with Langmuir, Freundlich and Langmuir–Freundlich (L–F) equations (Table 1).

Langmuir model considers a homogeneous surface with an infinite number of energetically equivalent sites, and a monolayer is formed on the adsorbent surface. Besides, adsorption sites are all equally available since the adsorption of a molecule is not influenced by the neighbor molecules [25]. The Freundlich equation considers that sorption occurs on inhomogeneous sorption sites and the L-F equation combines Freundlich and Langmuir models. Likewise, to select the most suitable model representing the experimental data, R^2 and the normalized standard deviation, Δg %, were calculated.

3 Results and Discussion

3.1 Materials' Characterization

Figure 2 presents the morphology of the materials used in this study. As can be noted, while CoAC presented a honeycomb-structured morphology, which is characteristic of the cell arrangement of the feedstock used (coconut residues), CeDC presented a contrasting morphology.

Figure 3a presents the N_2 sorption isotherms for both materials. According to IUPAC classification [29], CeDC exhibits a type IV isotherm with a hysteresis cycle classified as H1, which is characteristic of porous materials that have a very narrow pore size distribution. CoAC exhibits a type I isotherm. Hence, the composite-derived carbon is a mesoporous material, whereas the commercial activated carbon is a microporous one. CeDC yielded a BET surface area of 895 m^2 g^{-1} and a total pore volume of 1.99 cm^3 g^{-1}, while CoAC had a surface area of 1050 m^2 g^{-1} and a total

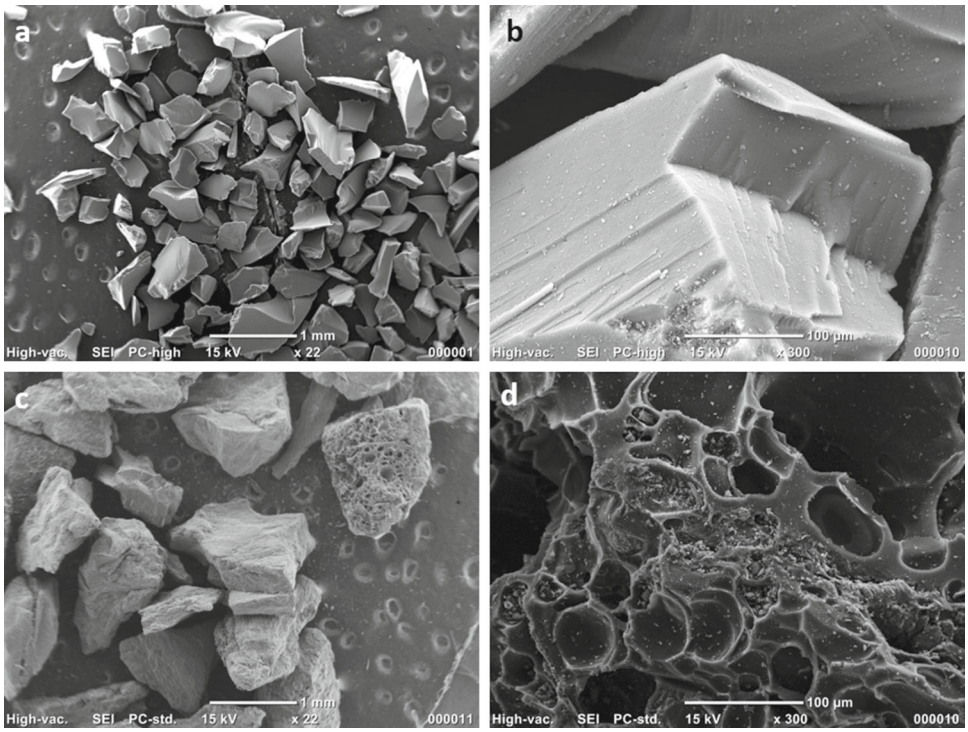

Fig. 2 SEM images for CeDC (**a, b**) and CoAC (**c**, **d**)

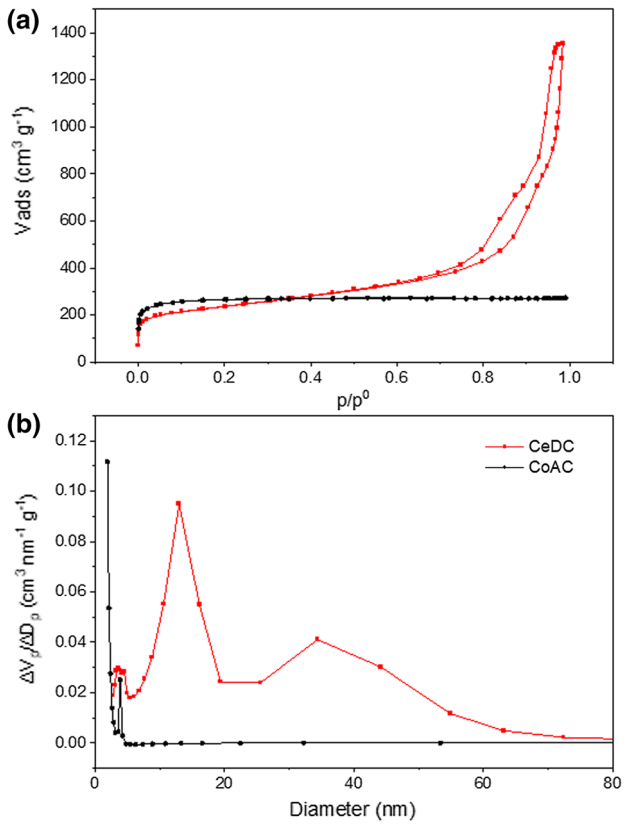

Fig. 3 N_2 sorption isotherms (**a**) and pore size distributions (**b**) for CeDC (red squares) and CoAC (black circles)

pore volume of 0.42 $cm^3\ g^{-1}$ (Table 2). Figure 3b presents the pore size distributions of the materials. CeDC exhibited a bimodal pore size distribution with diameters of 13.2 nm and 35 nm. The commercial carbon had a homogeneous pore distribution with a mean diameter of 4 nm. Therefore, the materials present different textural characteristics, which could account for differential sorption properties.

The zeta potential curves for CeDC and CoAC present a similar behavior: both carbons exhibited positive external surface electric charge below pH values of 2–3 and negative external surface electric charge above those pH values (Fig. 4). This could indicate that both materials present variable charges on their surface, as observed for other types of activated carbons [30] and biochars [31, 32]. CeDC was slightly less positive or negative, depending on the pH range, than CoAC, but this small difference should not be critical for the sorption process.

Table 3 shows the results of the Boehm titration for CeDC and CoAC, expressed as molecules per square nanometer of the surface, in order to better visualize differences in surface chemistry. The main acid surface groups were lactonic and carboxylic groups, for CeDC and CoAC, respectively. In both materials, the phenolic groups were the ones in the smallest amount. The total oxygen-containing surface functional groups, with values similar to those reported for a wood-derived carbon [33], were slightly higher for CoAC, and both were dominated by basic groups, being higher for CeDC. These differences on the surface functional groups could account for variable sorption capacities of the carbons,

Table 2 Textural parameters for CeDC and CoAC

	TPV ($cm^3\ g^{-1}$)	V_{micro} ($cm^3\ g^{-1}$)	V_{meso} ($cm^3\ g^{-1}$)	S_{BET} ($m^2\ g^{-1}$)	Mean size (nm)
CeDC	1.99	0.33	1.66	851	13.2 and 35
CoAC	0.42	0.4	–	1050	4

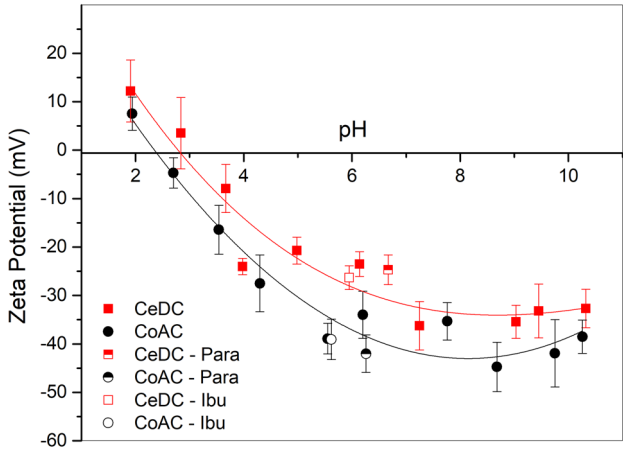

Fig. 4 Zeta potential curves for CeDC (full red squares) and CoAC (full black circles) samples before pollutants' sorption. Lines were included as tendency indicators. Half empty symbols represent data after paracetamol sorption and empty symbols after ibuprofen sorption

given that this functional groups could influence the sorption process.

The diffractogram of CeDC (Fig. 5a) presented the typical bands of an amorphous carbon: 25.6° 2θ (d002) and 43.6–43.7° 2θ (d100 and d101), indicating the presence of a non-crystalline pseudographitic structure [17]. CoAC reveals (Fig. 5a), in addition to a non-crystalline subgraphitic structure, diffraction peaks characteristic of silicon oxide (SiO_2, Reference code: 01-077-1060). Thus, as for textural analysis, both carbons present structural differences, which could account for the different sorption properties.

Regarding thermogravimetric analysis, both thermograms exhibit a considerable mass loss between 500 and 700 °C (Fig. 5b) that is accompanied by an exothermic process due to the C combustion reaction (peak/band observed in the DTA). CoAC left higher residue percentage (13.5% ash) than CeDC (7.51%), probably because CoAC sample contains silica, which is not affected by this thermal treatment.

3.2 Sorption of Emerging Pollutants

Paracetamol and ibuprofen removal percentages achieved under different pH and temperature conditions are presented in Fig. 6. For both drugs, the best removal percentage was achieved with no pH adjustment, namely, at 7.0 for paracetamol and 4.2 for ibuprofen. For paracetamol, a similar pH-dependent behavior for a coconut-based carbon has been reported [34]. For ibuprofen, Guedidi et al. reported higher removal percentages at low pH (pH = 3) on a commercial activated carbon [35]. As regards the temperature effect, paracetamol removal percentages increased with temperature, reaching a maximum at 25 °C for both materials. Ferreira et al. reported a similar trend for a coconut-based carbon [34]. For ibuprofen, while removal percentages did not differ between 15 and 25 °C for CeDC, CoAC presented the highest removal percentage at 25 °C. However in both cases, sorption resulted lower at 4 °C, indicating also the significant role of the temperature on the adsorption, as reported by Guedidi et al. [35]. Therefore, kinetic and equilibrium studies were carried out with no pH adjustment and at 25 °C.

3.2.1 Kinetic Studies

Figure 7 presents the kinetic experimental data for both materials, together with the different kinetic models, and Table 4 shows the calculated parameters, including the R^2 and Δg values. Considering the R^2 and Δg values, it can be concluded that the intraparticle equation best fitted the experimental data. In all cases, three fitting intervals were considered, indicating that at least three steps are involved in the sorption process: the first one is related to the instantaneous sorption onto the external surface of the material, the second step is

Table 3 Results of Boehm titration measurements for CoAC and CeDC

	Acid surface groups (molecules/nm^2)			Overall Acidity (mmol g^{-1})	Overall Basicity (mmol g^{-1})	All groups (mmol g^{-1})
	Carboxylic O=C–OH	Lactonic O=C–O	Phenolic – C–OH			
CeDC	0.047	0.060	0.012	0.12	0.32	0.44
CoAC	0.122	0.040	0.019	0.18	0.29	0.47

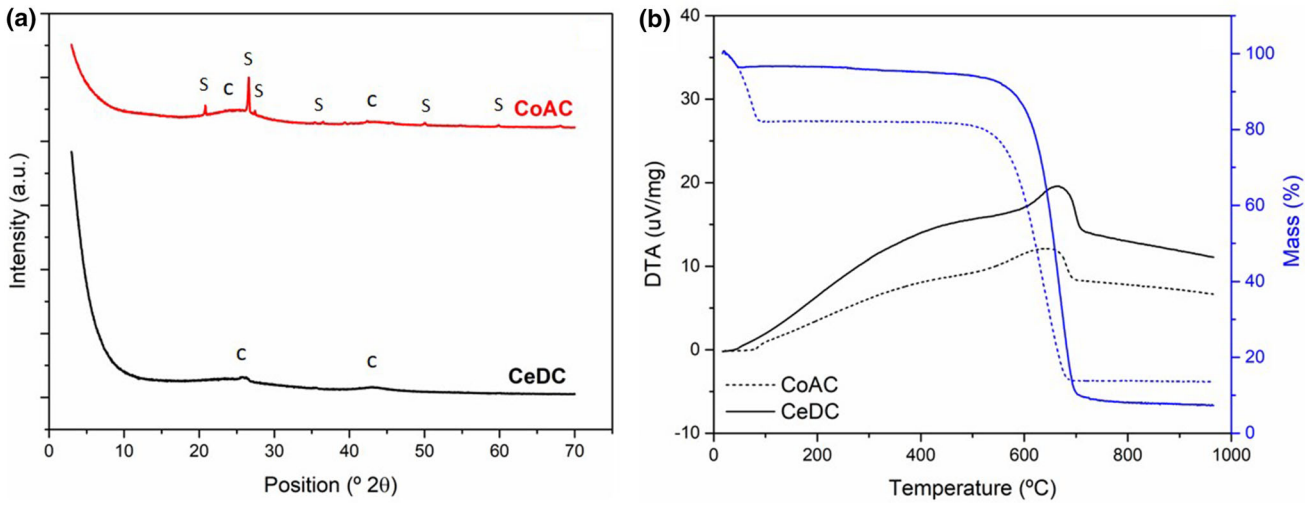

Fig. 5 **a** DRX (above, CoAC, down, CeDC, with S: silicon oxide, C: carbon) and **b** DTA-TG (straight line: CeDC, dotted line: CoAC)

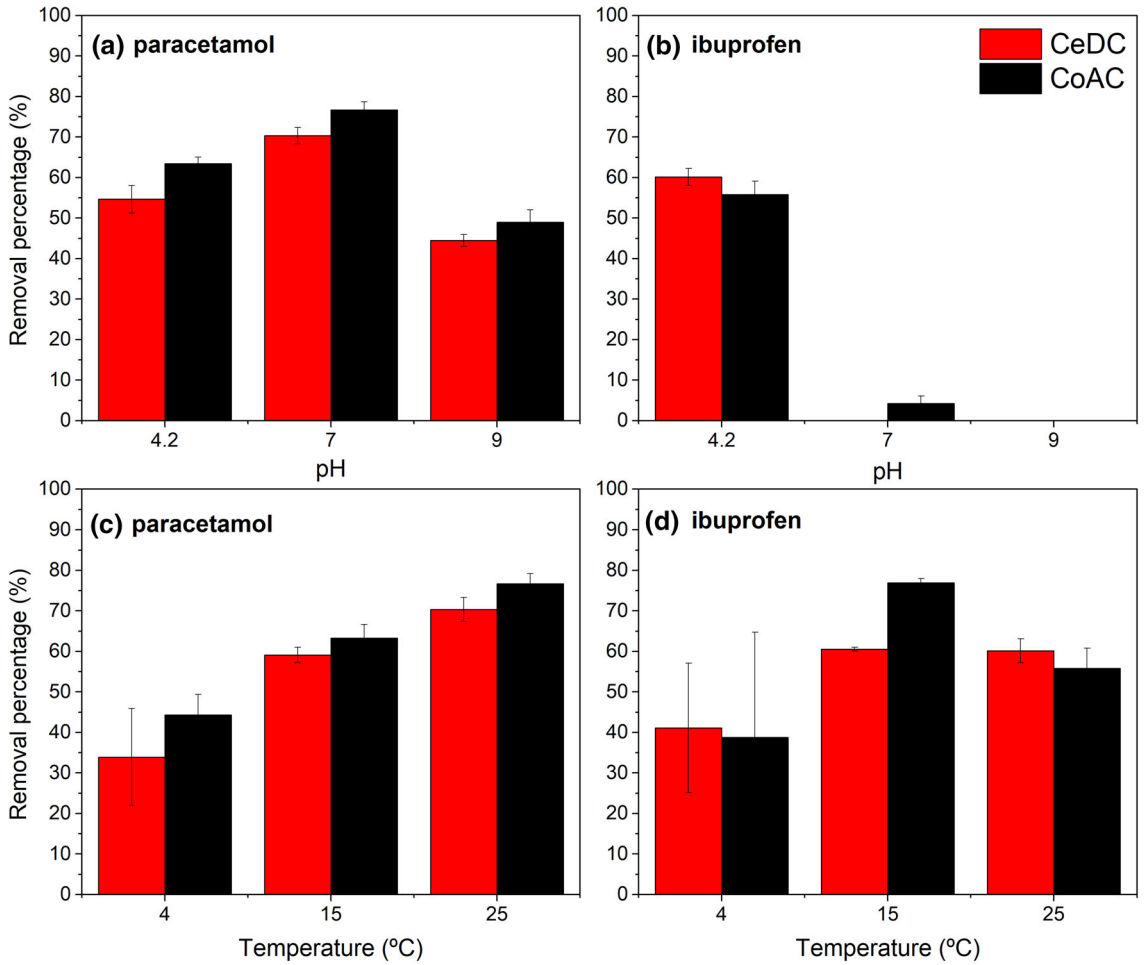

Fig. 6 Effect of pH (**a**, **b**) and temperature (**c**, **d**) on paracetamol and ibuprofen removal percentage for CoAC and CeDC (n = 2). Batch conditions: initial concentration = 200 mg L^{-1}, solid-to-liquid ratio = 1 g L^{-1} and constant stirring. For pH tests, temperature was kept at 25 °C and for temperature tests, pH was not adjusted (7.0 for paracetamol and 4.2 for ibuprofen)

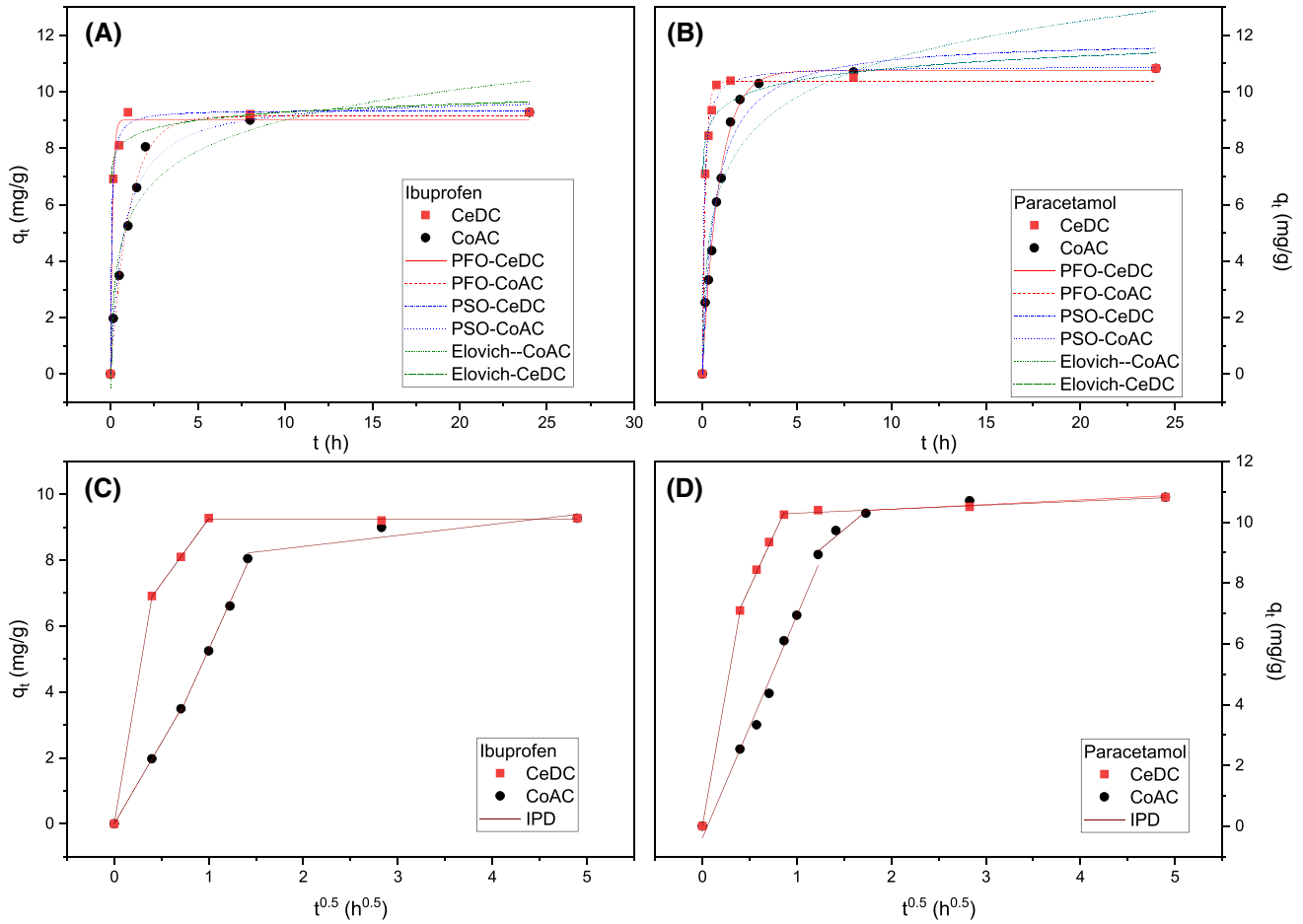

Fig. 7 Experimental kinetic data of CeDC and CoAC for ibuprofen (**a**, **c**) and paracetamol (**b**, **d**). Figures A and B include the fitting with PFO, PSO and Elovich models. Figures C and D correspond to qt versus $t^{0.5}$ for IPD model fitting. Batch conditions: initial concentration = 10 mg L^{-1}, solid-to-liquid ratio = 1 g L^{-1} and constant stirring at 25 °C

associated with a gradual sorption, where the intraparticle diffusion is controlled, and the third step is where the pollutant slowly enters trough the macropores to the micropores, with a relatively small adsorption rate [36].

The IPD rate constant for the first step, kp1, resulted higher for CeDC than CoAC, indicating a faster sorption process on the former over the material's surface. The attained kp1 for both drugs resulted similar, but for CoAC it was higher for paracetamol than for ibuprofen, indicating probably different affinity for the pollutant. For the second step, differences between the pollutants were observed. While for paracetamol CeDC presented a higher IPD rate constant than CoAC, for ibuprofen the trend was the opposite. The characteristics of the second step depend on systems variations, such as the concentration of the pollutant, the temperature and the sorbent's particle size [36]; therefore, the difference on the attained parameters seems to be related to the different sorbent material and pollutant characteristics, considering that experiments were performed under equal concentration and temperature conditions. It is relevant to mention that the time required to reach the equilibrium was higher for CoAC than CeDC, indicating that CeDC could be more suitable for household-level water filters.

3.2.2 Equilibrium Studies

Regarding the sorption isotherms, the Langmuir, Freundlich and L-F models were fitted to the experimental data (Fig. 8), and the maximum sorption capacities (q_m) for both materials were estimated (Table 5).

Paracetamol sorption on CeDC seems to be better represented by both the Freundlich equation and the L-F model, but on CoAC by L-F model. For ibuprofen, the L-F equation best represented the experimental data. These results indicate that the sorption of these pollutants occurs on inhomogeneous sorption sites, in agreement with what has already been reported for other carbons. Spesatto et al. [37] studied paracetamol sorption by a KOH-activated carbon and observed

Table 4 Fitted pseudo-first-order (PFO), pseudo-second-order (PSO), Elovich, and intraparticle diffusion (IPD) model kinetic parameters for the removal of paracetamol and ibuprofen by CoAC and CeDC

	Paracetamol		Ibuprofen	
	CeDC	CoAC	CeDC	CoAC
PFO				
q_e (mg g^{-1})	10.8 ± 0.2	10.4 ± 0.3	9.0 ± 0.3	9.0 ± 0.3
k_1·(g mg^{-1} min^{-1})	1.12 ± 0.06	6.1 ± 0.7	9 ± 2	0.93 ± 0.08
R^2	0.99	0.98	0.98	0.99
Δg	10.4	5.4	5.5	15.3
PSO				
q_e (mg g^{-1})	10.9 ± 0.2	11.9 ± 0.5	9.4 ± 0.2	9.9 ± 0.4
k_2·(g mg^{-1} min^{-1})	1.1 ± 0.2	0.13 ± 0.02	1.9 ± 0.4	0.14 ± 0.03
R^2	0.99	0.98	0.99	0.98
Δg	2.5	10.8	3.2	9.5
Elovich				
β	1.6 ± 0.5	0.52 ± 0.08	2.4 ± 0.9	0.63 ± 0.09
α	8E6 ± 4E6	22 ± 11	7.7E7 ± 6E8	17 ± 9
R^2	0.96	0.89	0.97	0.93
Δg	20.7	19.1	7.3	16.8
IPD				
C	0.00 ± 0.01	− 0.4 ± 0.3	0.00 ± 0.01	− 0.002 ± 0.005
k_{P1}	17.7 ± 0.8	7.3 ± 0.4	17.3 ± 0.6	4.93 ± 0.02
k_{P2}	6.8 ± 0.4	2.6 ± 0.7	3.94 ± 0.04	6.4 ± 0.3
k_{P3}	0.13 ± 0.02	0.15 ± 0.08	0.01 ± 0.02	0.3 ± 0.2
R^2	0.99/0.99/0.96	0.99/0.94/0.79	0.99/0.99/0.99	0.99/0.99/0.84
Δg	0.1/1.4/1.0	7.7/1.8/12.9	0.1/0.3/0.6	0.1/2.0/5.0
Average Δg	1.1	7.5	0.4	2.1

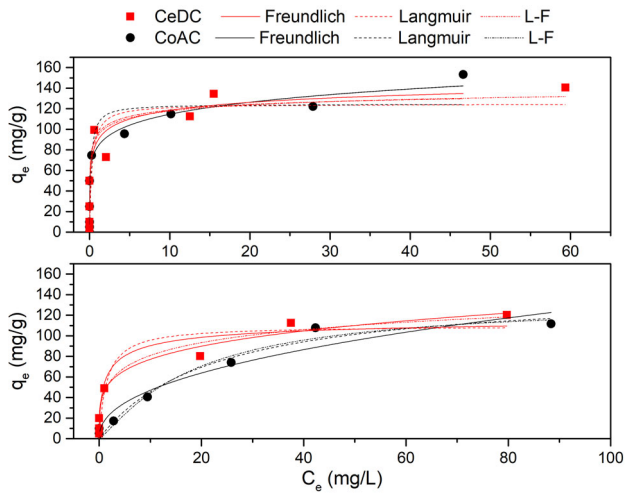

Fig. 8 Paracetamol (above) and ibuprofen (below) sorption isotherms for CoAC and CeDC in batch systems at 25 °C. Symbols correspond to experimental data and lines to the different fitted models

that the Langmuir–Freundlich hybrid model also best fitted the equilibrium data. For ibuprofen, Mestre et al. [9] and Debuy et al. [10] found that sorption isotherms showed a rather good agreement with Langmuir model, whereas Guedidi et al. [35] found that the Langmuir–Freundlich model best fitted the experimental adsorption data of modified activated carbon cloths at pH = 3. The best isotherm fittings indicate that sorption takes place on inhomogeneous sites, suggesting that aromatic rings are not equally available for pollutants during the sorption process, namely, some of them can be located at the external surface of the carbons, but other within the materials' pores.

Significant changes on zeta potential values after paracetamol and ibuprofen sorption processes were not observed (Fig. 4), indicating that the pollutant incorporation onto the carbons under the experimental conditions studied is not governed by electric interaction and, probably, the π-stacking interactions are responsible for the sorption. Several authors have highlighted the importance of π-stacking interaction between aromatic π-systems in organic compounds during the adsorption process [11]. The adsorption of organic compounds depends on different factors, including molecular features such as size, hydrophobicity, dissociation constant, surface functional groups, electrical charge, among others, which determine sorption mechanisms [38].

Table 5 Fitted models for experimental sorption data for paracetamol and ibuprofen by CoAC and CeDC

	Paracetamol		Ibuprofen	
	CeDC	CoAC	CeDC	CoAC
Langmuir				
K_L	3.3 ± 3.3	5.2 ± 4.5	0.67 ± 0.44	0.04 ± 0.01
q_m	124.6 ± 15.6	124.5 ± 13.0	109.8 ± 10.5	146.2 ± 16.2
R^2	0.77	0.80	0.89	0.96
Δg	17.8	16.2	9.9	41.7
Freundlich				
K_F	**88.3 ± 15.5**	83.0 ± 14.7	46.4 ± 10.3	17.1 ± 5.9
n	**8.7 ± 4.6**	7.1 ± 3.0	4.5 ± 1.2	2.27 ± 0.46
R^2	**0.82**	0.85	0.93	0.92
Δg	**18.6**	27.3	19.7	25.1
L–F				
q_m	159 ± 61	**150 ± 51**	**120 ± 21**	**133 ± 25**
K_a	3.3*	**5.2***	**0.67***	**0.06 ± 0.02**
n	0.3 ± 0.5	**0.3 ± 0.5**	**0.6 ± 0.5**	**1.2 ± 0.4**
R^2	0.83	**0.85**	**0.92**	**0.98**
Δg	21.6	**11.3**	**12.7**	**20.1**

*Indicates a fixed parameter for the fitting process. The bold font highlights the model that best represents the experimental data for each material

Both materials displayed a similar maximum sorption capacity for paracetamol, between 150 and 159 mg g^{-1} according to L–F model, and also for ibuprofen, with values around 125 mg g^{-1}. When the adsorptions of both pollutants are compared, it can be seen that the ceramic-derived carbon adsorbs more paracetamol than ibuprofen, namely 1.05 mmol g^{-1} and 0,58 mmol g^{-1}. This fact could be associated with the smaller molecular size of the paracetamol, which could allow paracetamol to enter more easily than ibuprofen into the material's pores, leading to a higher sorption capacity.

The assessment of the sorbent's efficiency is usually performed by comparing the maximum adsorption capacities predicted (q_m) with that of other materials for the same adsorbate [37]. Then, the sorption capacities obtained herein are in accordance with those obtained for other activated carbons reported in the literature (Table 6). The carbon developed in this study presents some of the highest sorption capacities for both pollutants, indicating that it could be a suitable sorbent material for emerging pollutants.

4 Conclusions

A ceramic-derived carbon, CeDC, was synthesized, and paracetamol and ibuprofen kinetics and sorption capacities were studied, using a commercial activated carbon as a reference material. Despite having a lower surface area, CeDC outperformed the activated carbon: paracetamol and ibuprofen removal from aqueous phase were faster, and CeDC matched the sorption capacity of the commercial activated carbon. The π-stacking interaction seemed to be responsible for the sorption process, and the isotherm fitting indicated that the available sorption sites could be located some on the external surface and others within the pore material. The ceramic-derived activated carbon has potential in the design of treatment systems to eliminate pharmaceuticals from water.

Table 6 Reported sorption capacities of carbons used for paracetamol and ibuprofen removal from aqueous phase

Feedstock	Treatment	pH	C_o (mg L^{-1})	q_m (mg g^{-1})	Reference
Paracetamol					
CeDC CoAC	– –	7	5–200	159 150	This study
Banana peels (750 °C)	–	2–10 (6)	0.5–200	57.3	[39]
Eucalyptus wood	– CO_2	7	5–180	14.4 98.2	[12]
Beetle kill pine timber	–	–	0–10	24.63	[40]
Jatoba fruits	Fe	3–10 (5)	25–500	234.4	[41]
Jatoba fruits	KOH	3–11 (5)	25–500	356.3	[37]
Sucrose-derived hydrochar	Vapor KOH	5	45–300	472 514	[42]
Olive pit	H_3PO_4	–	0.3–10	108–93	[43]
Wood	CO_2	–	41–1300	87.0	[44]
Peach pit	K_2CO_3	–	20–180	204.0	[45]
Ibuprofen					
CeDC CoAC	– –	4.2	5–200	120 133	This study
Chili seed	–	7	50–1000	12.78	[46]
Cloth	– NaOCl Heat	3, 7	5–100	491.9	[47]
Pinewood	–	3	25–100	10.74	[48]
Commercial AC	– H_2O_2 Heat	3, 7	5–100	160.0–185.2 146.6–159.9 190.7–256.2	[35]
Artemisia vulgaris	H_2SO_4 + heat	2–9	10–50	16.94	[10]
Cork powder	K_2CO_3 + steam K_2CO_3	2–11	20–120	106.4 112.4	[9]
PET	CO_2	2–11	20–120	138.9	[9]

Acknowledgements Amalia Bursztyn and Damian Benito acknowledge CONICET's doctoral scholarship, the Comisión de Investigaciones Científicas (CIC), who provided the infrastructure for the study, the *Unidad Productora de Medicamentos* of the Facultad de Ciencias Exactas (UNLP), who provided the drugs for the experiments, and Dr. Martín Nicolás Gatti for Boehm titrations. M.L. Montes acknowledges the financial support from the Argentine Ministry of Science (ANPCyT—PICT 2018-01536) and CONICET (PUE 066).

Author Contributions All authors contributed to the study conception and design. Material preparation, data collection and analysis were performed by ALBF, DEB and MLM. The first draft of the manuscript was written by ALBF and DEB. MBL and ANS supervised and commented on previous versions of the manuscript. All authors have read and approved the final manuscript.

Funding This study was financially supported by the projects X877 and X847 UNLP.

Data Availability The datasets generated during and/or analyzed during the current study are available from the corresponding author upon reasonable request.

Declarations

Conflict of interest The authors declare that they have no competing interests.

References

1. Becker, J.A.: Stefanakis, A.I.: Pharmaceuticals and personal care products as emerging water contaminants, Pharmaceutical sciences: breakthroughs in research and practice. (2017) 1457–1475. https://doi.org/10.4018/978-1-5225-1762-7.ch055
2. Lapworth, D.J.; Baran, N.; Stuart, M.E.; Ward, R.S.: Emerging organic contaminants in groundwater: a review of sources, fate and

occurrence. Environ. Pollut. **163**, 287–303 (2012). https://doi.org/10.1016/j.envpol.2011.12.034
3. Aldeguer Esquerdo, A.; Varo Galvañ, P.J.; Sentana Gadea, I.; Prats Rico, D.: Carbamazepine and diclofenac removal double treatment: oxidation and adsorption. IJERPH. **18**, 7163 (2021). https://doi.org/10.3390/ijerph18137163
4. Nassiri Koopaei, N.; Abdollahi, M.: Health risks associated with the pharmaceuticals in wastewater. DARU J Pharm Sci. (2017). https://doi.org/10.1186/s40199-017-0176-y
5. Ortúzar, M.; Esterhuizen, M.; Olicón-Hernández, D.R.; González-López, J.; Aranda, E.: Pharmaceutical pollution in aquatic environments: a concise review of environmental impacts and bioremediation systems. Front. Microbiol. **13**, 869332 (2022). https://doi.org/10.3389/fmicb.2022.869332
6. Hameed, B.H.; Din, A.T.M.; Ahmad, A.L.: Adsorption of methylene blue onto bamboo-based activated carbon: kinetics and equilibrium studies. J. Hazard. Mater. **141**, 819–825 (2007). https://doi.org/10.1016/j.jhazmat.2006.07.049
7. Alchouron, J.; Navarathna, C.; Chludil, H.D.; Dewage, N.B.; Perez, F.; Hassan, E.B.; Pittman, C.U., Jr.; Vega, A.S.; Mlsna, T.E.: Assessing South American *Guaduachacoensis* bamboo biochar and Fe3O4 nanoparticle dispersed analogues for aqueous arsenic(V) remediation. Sci. Total Environ. **706**, 135943 (2020). https://doi.org/10.1016/j.scitotenv.2019.135943
8. Omri, A.; Wali, A.; Benzina, M.: Adsorption of bentazon on activated carbon prepared from Lawsonia inermis wood: equilibrium, kinetic and thermodynamic studies. Arab. J. Chem. **9**, S1729–S1739 (2016). https://doi.org/10.1016/j.arabjc.2012.04.047
9. Mestre, A.S.; Pires, J.; Nogueira, J.M.F.; Parra, J.B.; Carvalho, A.P.; Ania, C.O.: Waste-derived activated carbons for removal of ibuprofen from solution: role of surface chemistry and pore structure. Biores. Technol. **100**, 1720–1726 (2009). https://doi.org/10.1016/j.biortech.2008.09.039
10. Dubey, S.P.; Dwivedi, A.D.; Sillanpää, M.; Gopal, K.: Artemisia vulgaris-derived mesoporous honeycomb-shaped activated carbon for ibuprofen adsorption. Chem. Eng. J. **165**, 537–544 (2010). https://doi.org/10.1016/j.cej.2010.09.068
11. Patel, M.; Chaubey, A.K.; Navarathna, C.; Mlsna, T.E.; Pittman, C.U.; Mohan, D.: Sorptive removal of pharmaceuticals using sustainable biochars. In: Mohan, D.; Pittman, C.U.; Mlsna, T.E. (Eds.) Sustainable biochar for water and wastewater treatment, pp. 395–427. Elsevier (2022). https://doi.org/10.1016/B978-0-12-822225-6.00006-3
12. Bursztyn Fuentes, A.L.; Canevesi, R.L.S.; Gadonneix, P.; Mathieu, S.; Celzard, A.; Fierro, V.: Paracetamol removal by Kon-Tiki kiln-derived biochar and activated carbons. Ind Crops Prod **155**, 112740 (2020). https://doi.org/10.1016/j.indcrop.2020.112740
13. Hudec, R.; Božeková, L.; Tisoňová, J.: Consumption of three most widely used analgesics in six European countries. J. Clin. Pharm. Ther. **37**, 78–80 (2012). https://doi.org/10.1111/j.1365-2710.2011.01256.x
14. Verlicchi, P.; Galletti, A.; Petrovic, M.; Barceló, D.: Hospital effluents as a source of emerging pollutants: an overview of micropollutants and sustainable treatment options. J. Hydrol. **389**, 416–428 (2010). https://doi.org/10.1016/j.jhydrol.2010.06.005
15. Geddes, L.: The fever paradox. New Sci. **246**, 39–41 (2020). https://doi.org/10.1016/S0262-4079(20)30731-4
16. Pandolfi, S.; Simonetti, V.; Ricevuti, G.; Chirumbolo, S.: Paracetamol in the home treatment of early COVID-19 symptoms: A possible foe rather than a friend for elderly patients? J. Med. Virol. **93**, 5704–5706 (2021). https://doi.org/10.1002/jmv.27158
17. Benito, D.E.; Lombardi, M.B.; Scian, A.N.: Mesoporous carbon from SiO2-C nanocomposite prepared with industrial raw materials: synthesis and characterization. Diam. Relat. Mater. **126**, 109047 (2022). https://doi.org/10.1016/j.diamond.2022.109047
18. Cychosz, K.A.; Thommes, M.: Progress in the physisorption characterization of nanoporous gas storage materials. Engineering **4**, 559–566 (2018). https://doi.org/10.1016/j.eng.2018.06.001
19. Boehm, H.P.: Surface oxides on carbon and their analysis: a critical assessment. Carbon **40**, 145–149 (2002). https://doi.org/10.1016/S0008-6223(01)00165-8
20. Oickle, A.M.; Goertzen, S.L.; Hopper, K.R.; Abdalla, Y.O.; Andreas, H.A.: Standardization of the Boehm titration: Part II. Method of agitation, effect of filtering and dilute titrant. Carbon **48**, 3313–3322 (2010). https://doi.org/10.1016/j.carbon.2010.05.004
21. Lagergreen, S.: Zur Theorie der sogenannten adsorption gelöster Stoffe. Zeitschr f Chem und Ind der Kolloide. **2**, 15–15 (1907). https://doi.org/10.1007/BF01501332
22. Ho, Y.S.; McKay, G.: Pseudo-second order model for sorption processes. Process Biochem. **34**, 451–465 (1999). https://doi.org/10.1016/S0032-9592(98)00112-5
23. Elovich, S.Y.; Larinov, O.G.: Theory of adsorption from solutions of non electrolytes on solid (I) equation adsorption from solutions and the analysis of its simplest form, (II) verification of the equation of adsorption isotherm from solutions. Izv. Akad. Nauk. SSSR Otd. Khim. Nauk. **2**, 209–216 (1962)
24. Weber, W.J., Jr.; Morris, J.C.: Kinetics of adsorption on carbon from solution. J. Sanit. Eng. Div. **89**, 31–59 (1963)
25. Langmuir, I.: The constitution and fundamental properties of solids and liquids. Part I. Solids. J. Am. Chem. Soc. **38**, 2221–2295 (1916). https://doi.org/10.1021/ja02268a002
26. Freundlich, H.: Über die Adsorption in Lösungen. Z. Phys. Chem. **57U**, 385–470 (1907). https://doi.org/10.1515/zpch-1907-5723
27. Foo, K.Y.; Hameed, B.H.: Insights into the modeling of adsorption isotherm systems. Chem. Eng. J. **156**, 2–10 (2010). https://doi.org/10.1016/j.cej.2009.09.013
28. Manohar, D.M.; Noeline, B.F.; Anirudhan, T.S.: Adsorption performance of Al-pillared bentonite clay for the removal of cobalt(II) from aqueous phase. Appl. Clay Sci. **31**, 194–206 (2006). https://doi.org/10.1016/j.clay.2005.08.008
29. Thommes, M.; Kaneko, K.; Neimark, A.V.; Olivier, J.P.; Rodriguez-Reinoso, F.; Rouquerol, J.; Sing, K.S.W.: Physisorption of gases, with special reference to the evaluation of surface area and pore size distribution (IUPAC Technical Report). Pure Appl. Chem. **87**, 1051–1069 (2015). https://doi.org/10.1515/pac-2014-1117
30. Tong, X.; Li, J.; Yuan, J.; Xu, R.: Adsorption of Cu(II) by biochars generated from three crop straws. Chem. Eng. J. **172**, 828–834 (2011). https://doi.org/10.1016/j.cej.2011.06.069
31. Mukherjee, A.; Zimmerman, A.R.; Harris, W.: Surface chemistry variations among a series of laboratory-produced biochars. Geoderma **163**, 247–255 (2011). https://doi.org/10.1016/j.geoderma.2011.04.021
32. Ndoun, M.C.; Elliott, H.A.; Preisendanz, H.E.; Williams, C.F.; Knopf, A.; Watson, J.E.: Adsorption of pharmaceuticals from aqueous solutions using biochar derived from cotton gin waste and guayule bagasse. Biochar. **3**, 89–104 (2021). https://doi.org/10.1007/s42773-020-00070-2
33. Salame, I.I.; Bandosz, T.J.: Surface chemistry of activated carbons: combining the results of temperature-programmed desorption, boehm, and potentiometric titrations. J. Colloid Interface Sci. **240**, 252–258 (2001). https://doi.org/10.1006/jcis.2001.7596
34. Cristina Ferreira, R.; Junior, O.; Carvalho, K.; Arroyo, P.; Barros, M.A.: Effect of solution pH on the removal of paracetamol by activated carbon of dende coconut mesocarp. Chem. Biochem. Eng. Q. J. **29**, 47–53 (2015). https://doi.org/10.15255/CABEQ.2014.2115
35. Guedidi, H.; Reinert, L.; Lévêque, J.-M.; Soneda, Y.; Bellakhal, N.; Duclaux, L.: The effects of the surface oxidation of activated carbon, the solution pH and the temperature on adsorption of ibuprofen. Carbon **54**, 432–443 (2013). https://doi.org/10.1016/j.carbon.2012.11.059

36. Wu, F.-C.; Tseng, R.-L.; Juang, R.-S.: Initial behavior of intraparticle diffusion model used in the description of adsorption kinetics. Chem. Eng. J. **153**, 1–8 (2009). https://doi.org/10.1016/j.cej.2009.04.042
37. Spessato, L.; Bedin, K.C.; Cazetta, A.L.; Souza, I.P.A.F.; Duarte, V.A.; Crespo, L.H.S.; Silva, M.C.; Pontes, R.M.; Almeida, V.C.: KOH-super activated carbon from biomass waste: insights into the paracetamol adsorption mechanism and thermal regeneration cycles. J. Hazard. Mater. **371**, 499–505 (2019). https://doi.org/10.1016/j.jhazmat.2019.02.102
38. Moreno-Castilla, C.: Adsorption of organic molecules from aqueous solutions on carbon materials. Carbon **42**, 83–94 (2004). https://doi.org/10.1016/j.carbon.2003.09.022
39. Patel, M.; Kumar, R.; Pittman, C.U.; Mohan, D.: Ciprofloxacin and acetaminophen sorption onto banana peel biochars: environmental and process parameter influences. Environ. Res. **201**, 111218 (2021). https://doi.org/10.1016/j.envres.2021.111218
40. Clurman, A.M.; Rodríguez-Narvaez, O.M.; Jayarathne, A.; De Silva, G.; Ranasinghe, M.I.; Goonetilleke, A.; Bandala, E.R.: Influence of surface hydrophobicity/hydrophilicity of biochar on the removal of emerging contaminants. Chem. Eng. J. **402**, 126277 (2020). https://doi.org/10.1016/j.cej.2020.126277
41. Spessato, L.; Cazetta, A.L.; Melo, S.; Pezoti, O.; Tami, J.; Ronix, A.; Fonseca, J.M.; Martins, A.F.; Silva, T.L.; Almeida, V.C.: Synthesis of superparamagnetic activated carbon for paracetamol removal from aqueous solution. J. Mol. Liq. **300**, 112282 (2020). https://doi.org/10.1016/j.molliq.2019.112282
42. Mestre, A.S.; Tyszko, E.; Andrade, M.A.; Galhetas, M.; Freire, C.; Carvalho, A.P.: Sustainable activated carbons prepared from a sucrose-derived hydrochar: remarkable adsorbents for pharmaceutical compounds. RSC Adv. **5**, 19696–19707 (2015). https://doi.org/10.1039/C4RA14495C
43. García-Mateos, F.J.; Ruiz-Rosas, R.; Marqués, M.D.; Cotoruelo, L.M.; Rodríguez-Mirasol, J.; Cordero, T.: Removal of paracetamol on biomass-derived activated carbon: modeling the fixed bed breakthrough curves using batch adsorption experiments. Chem. Eng. J. **279**, 18–30 (2015). https://doi.org/10.1016/j.cej.2015.04.144
44. Quesada-Peñate, I.; Julcour-Lebigue, C.; Jáuregui-Haza, U.J.; Wilhelm, A.M.; Delmas, H.: Degradation of paracetamol by catalytic wet air oxidation and sequential adsorption—catalytic wet air oxidation on activated carbons. J. Hazard. Mater. **221–222**, 131–138 (2012). https://doi.org/10.1016/j.jhazmat.2012.04.021
45. Cabrita, I.; Ruiz, B.; Mestre, A.S.; Fonseca, I.M.; Carvalho, A.P.; Ania, C.O.: Removal of an analgesic using activated carbons prepared from urban and industrial residues. Chem. Eng. J. **163**, 249–255 (2010). https://doi.org/10.1016/j.cej.2010.07.058
46. Ocampo-Perez, R.; Padilla-Ortega, E.; Medellin-Castillo, N.A.; Coronado-Oyarvide, P.; Aguilar-Madera, C.G.; Segovia-Sandoval, S.J.; Flores-Ramírez, R.; Parra-Marfil, A.: Synthesis of biochar from chili seeds and its application to remove ibuprofen from water. Equilibrium and 3D modeling. Sci. Total Environ. **655**, 1397–1408 (2019). https://doi.org/10.1016/j.scitotenv.2018.11.283
47. Guedidi, H.; Reinert, L.; Soneda, Y.; Bellakhal, N.; Duclaux, L.: Adsorption of ibuprofen from aqueous solution on chemically surface-modified activated carbon cloths. Arab. J. Chem. **10**, S3584–S3594 (2017). https://doi.org/10.1016/j.arabjc.2014.03.007
48. Essandoh, M.; Kunwar, B.; Pittman, C.U.; Mohan, D.; Mlsna, T.: Sorptive removal of salicylic acid and ibuprofen from aqueous solutions using pine wood fast pyrolysis biochar. Chem. Eng. J. **265**, 219–227 (2015). https://doi.org/10.1016/j.cej.2014.12.006